Electrophysiological and Morphological Properties of Neurons Acutely Isolated from the Rostral Gustatory Zone of the Rat Nucleus of the Solitary Tract

Junhui Du[1] and Robert M. Bradley[1, 2]

[1]Department of Biologic and Materials Sciences, School of Dentistry, University of Michigan, Ann Arbor, MI 48109-1078 and [2]Department of Physiology, Medical School, University of Michigan, Ann Arbor, MI 48109-0622, USA

Correspondence to be sent to: Robert M. Bradley, Department of Biologic and Materials Sciences, 6228 School of Dentistry, University of Michigan, Ann Arbor, MI 48109-1078, USA

Abstract

The biophysical and morphological characteristics of acutely isolated neurons from the rostral nucleus of the solitary tract (rNST) were investigated under current clamp conditions and compared with the results obtained from neurons recorded in brain slices. The passive membrane properties of the isolated neurons were similar to rNST neurons in brain slices and the neurons maintained their morphological characteristics although their dendritic tree was truncated. The isolated neurons also retained their characteristic repetitive firing properties. In addition we also noted developmental changes in the intrinsic membrane properties of the isolated neurons, such as a shortening in action potential duration, decrease in membrane time constant and input resistance, that occurred when these parameters were compared in neurons isolated from young (5–10 days) and older animals. These enzymatically dispersed neurons therefore retained both the membrane properties and morphology observed in the intact brainstem and *in vitro* brain slice preparation. The use of this isolated neuron preparation provides a basis for further study of rNST neurobiology.
Chem. Senses 21: 729–737, 1996

Introduction

Until recently electrophysiological studies of the first relay in the central taste pathway—the rostral nucleus of the solitary tract (rNST)—have used the technique of extracellular recording *in vivo*. Combined with neuroanatomical techniques and tracing of central pathways, these methodologies have provided a wealth of information on termination patterns of afferent taste fibers as well as the response properties and morphology of second order taste neurons (see e.g. Doetsch and Erickson, 1970; Travers and Smith, 1979; Hamilton and Norgren, 1984; Ogawa *et al.*, 1984; Whitehead, 1988; Vogt and Mistretta, 1990; Mistretta and Labyak, 1994). However, these techniques can provide only a limited understanding of the basic biophysical, pharmacological, synaptic and ionic properties of neurons involved in processing taste information.

The use of the *in vitro* brain slice preparation has permitted us to study the properties of individual neurons in rNST and to examine the synaptic properties of the primary afferent synapse (Bradley and Sweazey, 1992; King and Bradley, 1994; Tell and Bradley, 1994; Wang and Bradley,

© Oxford University Press

Downloaded from http://chemse.oxfordjournals.org/ by guest on October 3, 2012

1995). The rNST can be easily visualized in brain slices when transilluminated, but unlike other brain areas such as the hippocampus, which are laminated, it is not possible to position the electrode in a defined cell population. Thus, to determine the morphology of the neuron being recorded, it is necessary to fill the neuron with a label and subsequently reconstruct the neuron, which is a time-consuming process. An additional problem presented by the brain slice preparation is that the projection pattern of the neuron is not known and often cannot be determined later after neuron labeling. A further limitation of the brain slice preparation is that a considerable time is needed to superfuse pharmacological agents over the slice because the agent has to diffuse to the neuron. Thus, it is often necessary to make long stable recordings from a neuron to be able to fully characterize its pharmacological properties. To overcome these problems we have isolated neurons of the rNST using methods similar to those used by investigators of the caudal, non-gustatory NST (Nakagawa *et al.*, 1990). Isolated neurons permit the rapid structure–function analysis of neurons as well as facilitate neuropharmacological analysis of neuron responses to transmitter agonists and antagonists. In this report we present details of the isolation process and describe the biophysical and morphological properties of the acutely isolated neurons.

Materials and methods

Cell preparation

Neurons were isolated from brain slices of rats aged 7–25 days. The preparation of brain slices has already been described in detail (Bradley and Sweazey, 1992). Briefly, rats were anesthetized with sodium pentobarbital (50 mg/kg) and decapitated. The whole brain, including the cervical spinal cord, was rapidly removed and placed in ice-cold HEPES buffer containing (in mM) 124 NaCl, 5 KCl, 5 $MgCl_2$, 10 sodium succinate, 15 dextrose, 15 HEPES and 2 $CaCl_2$, and gassed with O_2. The pH was adjusted to 7.4 with 1 M NaOH. Horizontal 300 μm thick brainstem slices were cut on a Vibratome and placed in a holding chamber filled with the HEPES buffer at room temperature.

After incubating the slices for 1.0–1.5 h, the left and right rNST were microdissected from the slices and transferred to the HEPES buffer containing 0.5% protease (Sigma type 23) for 30 min at 37°C. The rNST was then triturated with a series of progressively smaller diameter, fire-polished Pasteur pipettes to produce a suspension of dissociated neurons which were placed on a poly-L-lysine-coated coverslip in a 35 mm diameter plastic petri dish. Once the cells adhered to the coverslip, they were superfused with oxygenated HEPES buffer.

Neurons were isolated from the NST in an area located rostral to the point where the medial border of the NST separates from the lateral edge of the fourth ventricle. This region is innervated by gustatory nerves (Hamilton and Norgren, 1984) and therefore contains principal neurons and interneurons involved in processing gustatory, thermal and somatosensory information.

Electrophysiological recording

Patch electrodes, pulled in two stages from 1.5 mm OD borosilicate filament glass, were filled with a solution containing (in mM) 130 potassium gluconate, 10 HEPES, 10 EGTA, 1 $MgCl_2$, 1 $CaCl_2$ and 2 ATP. The pipette solution was adjusted to a pH of 7.2 with KOH and had an osmolarity of 275–292 mOsm. Electrode resistance was between 5 and 8 MΩ. In some experiments 0.5% Lucifer yellow was added to the filling solution (Figure 1).

The Petri dish containing the neurons was mounted on the stage of an inverted microscope equipped with epifluorescence and Hoffman modulation optics. Electrodes were manipulated under visual control and conventional patch-clamp recordings were performed in whole cell mode (Hamill *et al.*, 1981).

Current-clamp recordings were made using an Axoclamp 2A amplifier (Axon Instruments). Bridge balance was carefully monitored throughout the experiments and adjusted when necessary. The junction potential due to potassium gluconate (10 mV) was subtracted from the recorded membrane voltages (Standen and Stanfield, 1992). Criteria for a successful recording included a minimum of 10 min recording time with a stable resting membrane potential of >–40 mV, an action potential amplitude >50 mV and a neuron input resistance >120 MΩ.

To compare the results of the present study with those we had previously obtained in brain slices (Bradley and Sweazey, 1992) we separated the neurons into four different groups on the basis of their responses to a current injection pulse protocol. Group I–III neurons respond to a long (1200 ms) depolarizing current pulse with a regular train of action potentials. Group IV neurons respond to this same depolarizing pulse with a transient burst of action potentials followed by prolonged inactivation of the firing activity.

Downloaded from http://chemse.oxfordjournals.org/ by guest on October 3, 2012

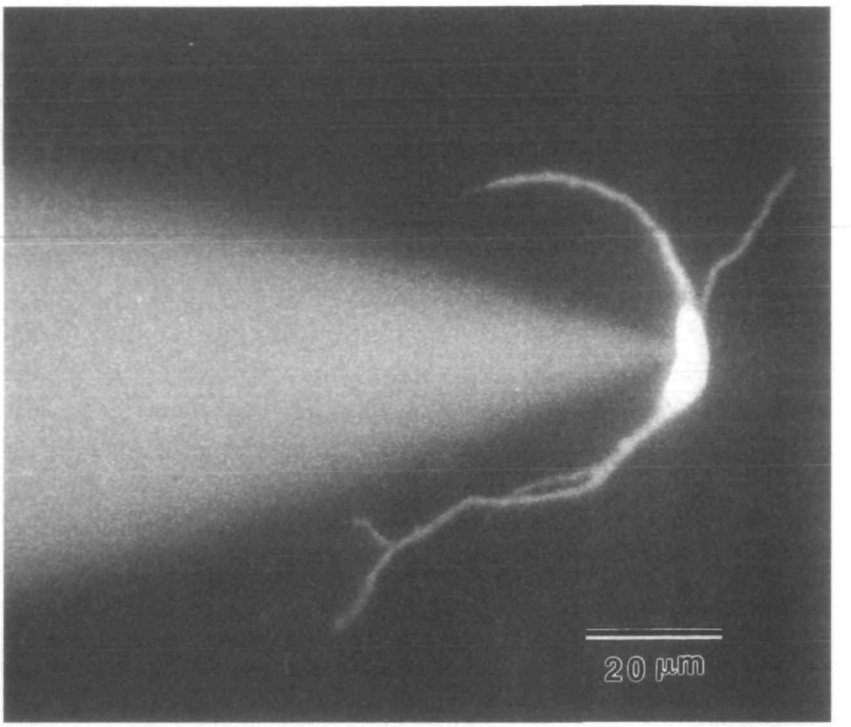

Figure 1 Photomicrograph of a dissociated elongate neuron during recording with a patch electrode containing 0.5% Lucifer Yellow.

When the long depolarizing pulse is preceded by membrane hyperpolarization the regular train of action potentials produced by the depolarization is altered in group I and II neurons. Membrane hyperpolarization of group I neurons changes the regular discharge pattern into a train of irregularly occurring spikes. Hyperpolarization of group II neurons either delays the occurrence of the first action potential or increases the length of the first interspike interval in the action potential train produced by membrane depolarization. Hyperpolarization least affects the discharge pattern of group III neurons.

The results are based on recordings from 59 neurons. All electrophysiological data were acquired and analyzed using pCLAMP software (Axon Instruments). A photographic record was made of each neuron which was later used to make measurements of anatomical characteristics. The photographs were taped to a bit pad interfaced to a computer and analyzed using morphometric software (Eutectic Electronics). For each neuron we measured somal diameter, perimeter, area, form factor, dendritic length and number of primary dendrites. Somal form factor is a measure of the roundness of the cell body, where 1 indicates a perfect circle and 0 indicates a line. The formula to calculate this parameter is: $(4\pi \times \text{area})/\text{perimeter}^2$.

The neurons were categorized into different types using previously established criteria in which neurons were classified as elongate, multipolar or ovoid by visual and morphometric analysis of neuronal features (Lasiter and Kachele, 1988; Whitehead, 1988; King and Hill, 1993; King and Bradley, 1994; Mistretta and Labyak, 1994). Multipolar neurons were distinguished by their triangular or polygonal somata with three to five primary dendrites originating almost equidistantly from the cell body. Elongate neurons had two primary dendrites that originated from opposite poles of the cell body and a somal shape that varied from spherical to fusiform. Ovoid neurons had spherical to ovoid somata with two to five thin primary dendrites. Statistical analysis was performed using the Microcal Origin program (MicroCal Software, Inc.). The numerical value are given as mean ± SEM, and statistical significance ($P \leq 0.05$) was assessed using paired *t*-tests.

Results

Morphological characteristics of the isolated neurons

The soma of the isolated neurons had a mean diameter of 17.9 ± 0.5 μm, an average area of 256 ± 15 μm^2, a perimeter of 70.1 ± 3.1 μm and a mean form factor of 0.69 ± 0.02. The

Downloaded from http://chemse.oxfordjournals.org/ by guest on October 3, 2012

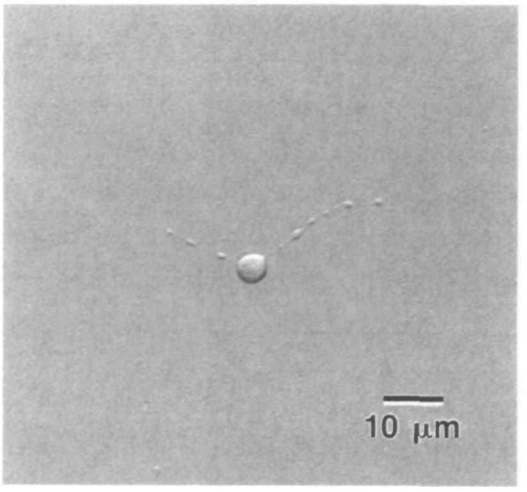

Figure 2 Photomicrograph of an acutely isolated rNST neuron showing dendritic swellings giving it a beaded appearance.

mean number of primary dendrites was 3.4 ± 0.2, and the total dendritic length ranged from 18 to 485 μm. Some neurons (7%) had dendrites with frequent swellings along their length, giving them a beaded appearance. This was most often observed on the thinner dendritic processes of ovoid neurons (Figure 2).

All the neurons were classified into multipolar, elongate and ovoid neurons (Figure 3) based on criteria we established previously (King and Bradley, 1994). Cell types can usually be identified from their dendritic pattern. Multipolar neurons have the most dendrites which are moderately branched (Figure 3A), elongate neurons have two major dendrites (Figure 3B) and ovoid neurons have the shortest dendrites which are relatively unbranched (Figure 3C). Several other morphological properties were significantly different among the three groups (Table 1). For example, multipolar neurons had the most primary dendrites, the longest dendritic tree and the largest cell bodies. Ovoid neurons had the smallest dendritic tree and the smallest, most spherical cell body. In an additional 20 animals we determined the relative occurrence of the three cell types by counting the numbers of dispersed multipolar, elongate and ovoid neurons (a total of 2520 neurons). Most of the dispersed neurons were ovoid neurons (60.9%); the next most frequently encountered type was multipolar neurons (23.5%), while elongate neurons were the least frequently counted (15.5%) (Table 1).

Biophysical properties of the isolated neurons

Resting membrane potentials ranged from –46.6 to –74.2 mV, with a mean of –56 ± 0.9 mV. Action potential amplitudes were between 50 and 112 mV (mean = 65 ± 1.7 mV), with a mean duration measured at half amplitude of 3.5 ± 0.2 ms. Input resistance ranged from 161 to 635 MΩ and averaged 399 ± 13.1 MΩ. Membrane time constants ranged from 10 to 89 ms and averaged 32.7 ± 1.5 ms. The membrane biophysical properties of the three morphological types of rNST neurons were similar (Table 2).

Since the ages of the animals used in this study were similar to the ages of the animals we had previously used to study development of the intrinsic membrane properties of rNST neurons in brain slices (Bao *et al.*, 1995) we could directly compare the results of both studies. We therefore separated the animals into four age groups: 5–10 days (n = 4), 11–15 days (n = 13), 16–20 days (n = 34) and 21–25 days (n = 8). The resting membrane potential and action potential amplitude did not alter over development. However, input resistance, membrane time constant and action potential duration all decreased substantially during development (Figure 4). These results are similar to those we have already reported in our previous study using brain slices.

Neurons were separated into repetitive firing pattern groups using long depolarizing current injections either alone or preceded by a hyperpolarizing current injection. Neurons with the repetitive firing characteristics of groups II (n = 5), III (n = 21) and IV (n = 33) were recorded. However, neurons with group I repetitive firing characteristics were not encountered.

Examples of the repetitive firing patterns of a multipolar, elongate and ovoid neuron are shown in Figure 3 (D–F respectively). The multipolar neuron (Figure 3A) had a group II firing pattern (Figure 3D), the elongate neuron (Figure 3B) a group III pattern (Figure 3E) and the ovoid neuron (Figure 3C) a group IV pattern (Figure 3F). Although no firing pattern was exclusive to all neurons in a morphological group, there were differences in the proportion of multipolar, elongate and ovoid neurons in each of the biophysical groups. The majority of multipolar neurons had a group IV response (52.8%), but other multipolar neurons exhibited the firing characteristics of group III (36.1%) and group II (8.3%). Elongate neurons had either group IV (66.7%) or group III (33.3%) firing patterns. Most ovoid neurons had a group IV response (52.9%), but some responded with group II (17.6%) or group III (29.4%) firing patterns (Figure 5).

Downloaded from http://chemse.oxfordjournals.org/ by guest on October 3, 2012

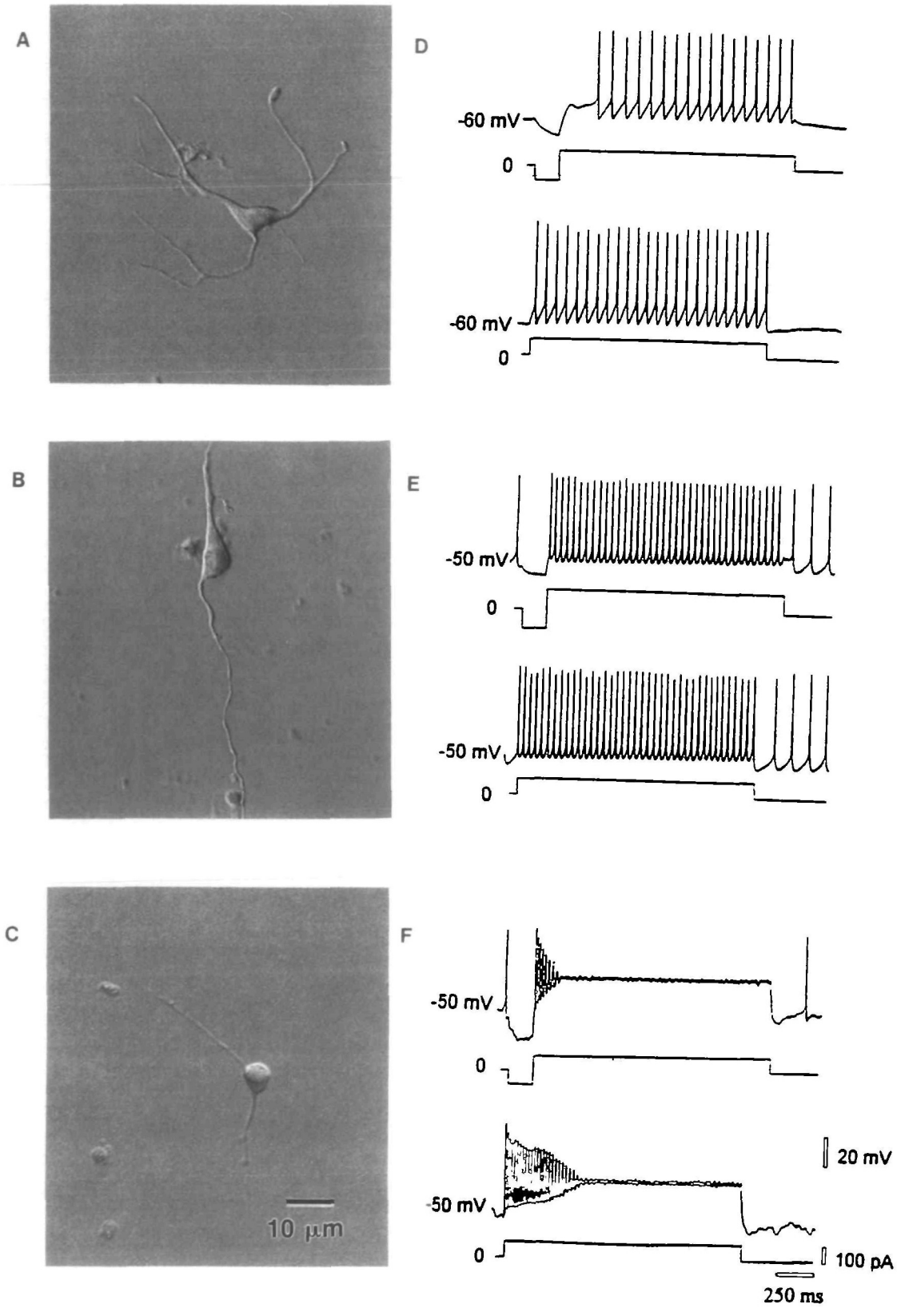

Figure 3 Photomicrographs of isolated multipolar **(A)**, elongate **(B)** and ovoid **(C)** neurons. Repetitive discharge characteristics of the neurons are illustrated in A–C to a long depolarizing current injection either alone or preceded by a short hyperpolarizing current injection. The multipolar neuron (A) had a group II pattern of response **(D)**, the elongate neuron (B) had a group III pattern of response **(E)** and the ovoid neuron (C) had a group IV pattern of response **(F)**.

Downloaded from http://chemse.oxfordjournals.org/ by guest on October 3, 2012

Table 1 Morphological properties of multipolar, elongate and ovoid neurons

	Multipolar (n = 36)	Elongate (n = 6)	Ovoid (n = 17)
Primary dendrite number	4.1 ± 0.2^{e,o}	2.4 ± 0.4^{m}	2.3 ± 0.1^{m}
Total dendritic length (μm)	142.7 ± 17.1^{e,o}	102.0 ± 19.2^{m,o}	80.0 ± 10.4^{m,e}
Somal area (μm^2)	289.5 ± 19.0^{o}	256.2 ± 37.7^{o}	169.9 ± 10.9^{m,e}
Somal mean diameter (μm)	19.1 ± 0.7^{o}	17.9 ± 1.2^{o}	14.7 ± 0.5^{m,e}
Soma form factor	0.62 ± 0.02^{o}	0.71 ± 0.10	0.83 ± 0.01^{m}

Data are means ± SEM. Superscript letters indicate a significant difference from the multipolar (m), elongate (e) and/or ovoid (o) groups.

Table 2 Biophysical properties of multipolar, elongate and ovoid neurons

	Multipolar (n = 36)	Elongate (n = 6)	Ovoid (n = 17)
Action potential amplitude (mV)	65.9 ± 2.4	66.7 ± 8.6	61.5 ± 1.9
Action potential half-width (ms)	3.4 ± 0.2	4.1 ± 0.7	3.5 ± 0.4
Input resistance (MΩ)	383.7 ± 18.7	376.3 ± 33.9	425.6 ± 23.2
Resting membrane potential (mV)	−54.8 ± 1.1	60.4 ± 3.5	−57.6 ± 1.7
Time constant (ms)	33.1 ± 2.4	30.6 ± 1.7	32.6 ± 1.8

Data are means ± SEM.

Discussion

The goal of this study was to evaluate the suitability of enzymatically dispersed neurons of the rNST for the study of their biophysical properties and morphological characteristics. Our study shows that it is possible to isolate rNST cells and obtain high quality whole cell recordings. Moreover, we were able to obtain successful recordings from neurons from postnatal day 7 to postnatal day 25. This will allow us to examine developmental changes in these neurons as we have already shown that rNST neurons have obtained adult passive properties by 25 days postnatal (Bao *et al.*, 1995).

The action potentials and passive membrane properties are similar to those we have already reported for rNST neurons recorded using whole cell recordings in brain slices (Bradley and Sweazey, 1992). This suggests that the isolation procedure does not alter the characteristics of these cells. In addition, we also noted developmental changed in the intrinsic membrane properties of the isolated neurons, such as a shortening in action potential duration, decrease in membrane time constant and input resistance, that occurred when these parameters were compared in neurons isolated from young (5–10 days) and older animals. We have already described a similar developmental change using rNST brain slices from early postnatal and young adult rats (Bao *et al.*, 1995), indicating the utility of the isolated neurons for the study of developmental processes in the rNST.

The isolated neurons also responded to long depolarizing current injection pulses, either alone or preceded by a hyperpolarizing pulse in a way similar to rNST neurons recorded in brain slices. Neurons could be separated into groups II, III and IV based on repetitive firing patterns as described previously (Bradley and Sweazey, 1992), further indicating that these neurons are not damaged by the isolation process. We were not able to record neurons with a group I response pattern. However, this type of response pattern is the least frequently encountered in recordings from brain slices (King and Bradley, 1994) and therefore the chances of recording from isolated neurons with a group I pattern may be smaller than the other groups. It is also possible that the group I response pattern is lost during the process of isolation due to shortening of the dendritic tree or loss of synaptic connections.

Not only are the neurons biophysically similar to those we have recorded in brain slices, their morphology is also retained after isolation. The three basic types of neuron described by us in brain slices (King and Bradley, 1994) and by others using the Golgi technique *in vivo* (Davis and Jang; 1988; Lasiter and Kachele, 1988; Whitehead, 1988; King and Hill, 1993; Mistretta and Labyak, 1994) are easily distinguished in the isolated preparation. The proportions of elongate, multipolar and ovoid neurons identified in brain slices (King and Bradley, 1994) and in the isolated preparation are similar. Ovoid neurons are the most numerous (48.3% brain slice, 60.9% dissociated preparation), multipolar cells make up 36.2% in slices and 23.5% when dissociated, and elongate neurons are the most

Downloaded from http://chemse.oxfordjournals.org/ by guest on October 3, 2012

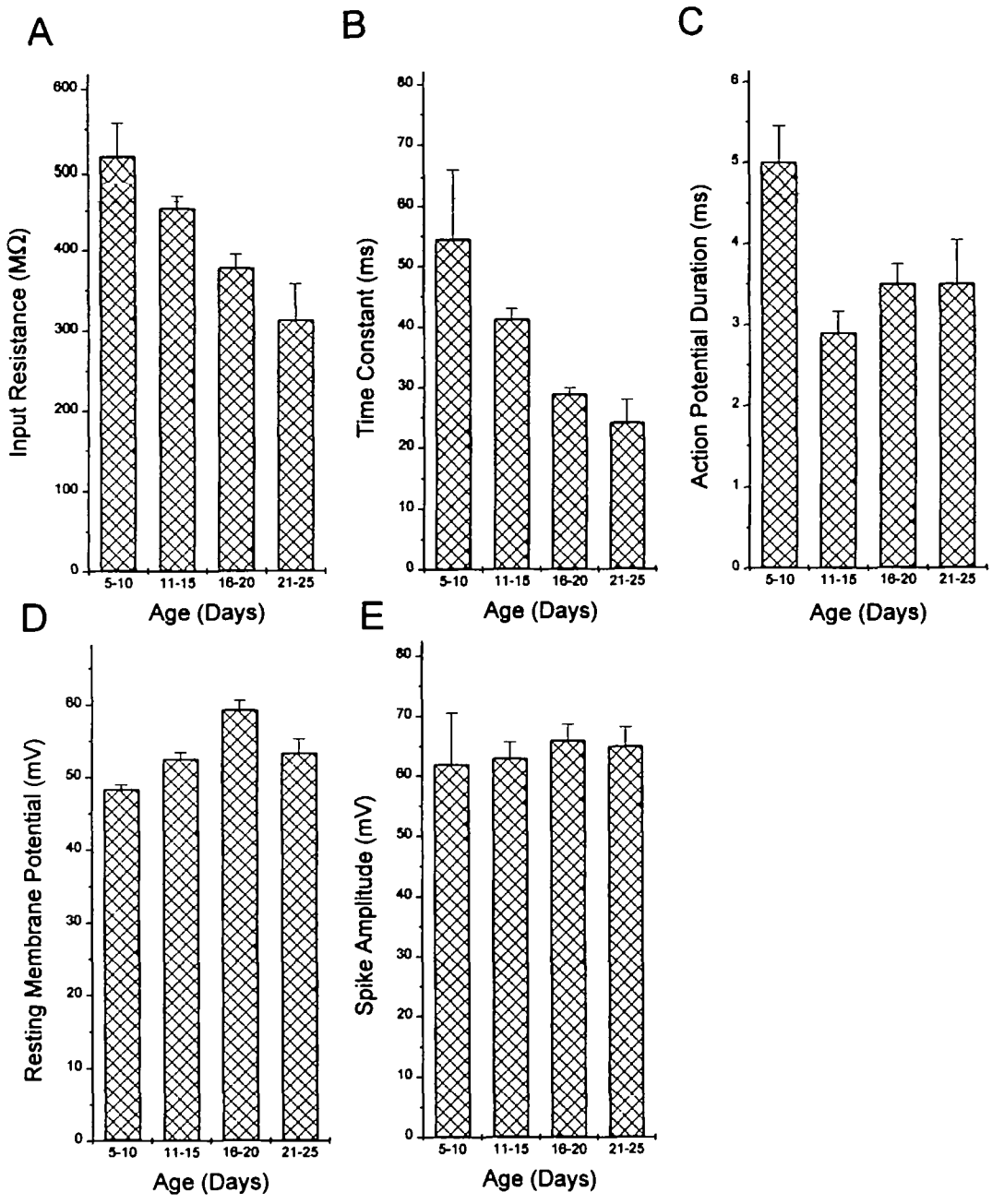

Figure 4 Passive membrane properties of the isolated rNST neurons at four different postnatal ages. Data are presented as means and SEMs. **(A–C)** Input resistance, membrane time constant and action potential duration all decrease during development. **(D, E)** Resting membrane potential and spike amplitude do not alter during development.

rarely encountered in slices (15.5%) and when dissociated (15.6%). Differences in the percentages between the results obtained using brain slices and the current study can probably be accounted for by the number of cells sampled, which was only 58 in the brain slices and 2520 in the dissociated neurons.

Although the general morphometric characteristics of the three neuron types are similar to those we have described in brain slices (King and Bradley, 1994), the dendritic trees in the dissociated neurons are truncated during the enzymatic separation. The mean total dendritic length for elongate, multipolar and ovoid neurons in brain slices was 1960, 2629 and 1377 μm respectively (King and Bradley, 1994), and 102, 143 and 80 μm in the dissociated cells (Table 1). Despite this considerable reduction in the dendritic tree, it is still possible to distinguish the different morphological types of neuron.

Downloaded from http://chemse.oxfordjournals.org/ by guest on October 3, 2012

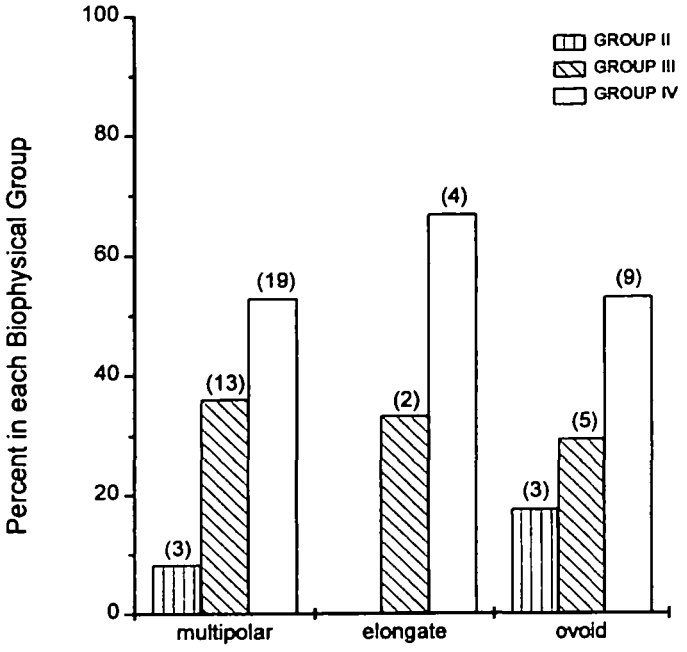

Figure 5 Graph of the proportion of multipolar, elongate and ovoid neurons having the repetitive firing characteristics of groups II, III and IV. The number of neurons represented by each bar is indicated above each bar.

However, loss of the distal dendrites may influence functional characteristics if there are differences in the distributed synaptic receptors and ion channels between the soma and the distal dendrites. These differences have been demonstrated in several neuron populations. For example, $GABA_B$ receptors are concentrated on the dendrites of hippocampal pyramidal cells, while $GABA_A$ receptors are located principally on the cell soma (Newberry and Nicoll, 1985). Thus, loss of the distal dendrites on the rNST neurons could significantly reduce a receptor population and thus alter the neuropharmacological properties of the isolated neurons.

On the other hand, there are some advantages in having a reduced dendritic tree. In particular, the isolated neurons would be better suited to voltage clamp experiments because the loss of the distal dendrites results in higher membrane input resistance, resulting in a reduction in series resistance error and problems with space clamp (Kay and Wong, 1986). Under these conditions voltage- and drug-activated currents can be accurately determined and their modulation by intra- or extracellularly applied agents measured.

A further difference between the response characteristics of the brain slice and isolated rNST neurons is the distribution of the repetitive response groups among the different morphological types. In brain slices the group II response pattern predominated (King and Bradley, 1994) while the group IV type of pattern is most often encountered in the isolated neurons. While this difference may be due to the isolation process, it may also be related to the differing proportions of the morphological cell types studied. In brain slices most of the neurons studied were ovoid neurons while the majority were multipolar neurons in the current study (Table 1). The type of neuron recorded in brain slices is somewhat random since it is not possible to distinguish different cell populations in transilluminated slices. However, it is very easy to study particular types of neuron in the isolated cell preparation and therefore make detailed analyses of a single cell type such as the ovoid cells, which are believed to be interneurons (Lasiter and Kachele, 1988).

In summary, we have described an isolated neuron preparation of rNST that preserves the repetitive firing characteristics and morphology of the neurons observed *in vivo* and in a brain slice preparation. This preparation will facilitate rapid application and removal of neurotransmitter agonists and antagonists, and permit direct correlations between functional and morphological characteristics of these neurons. By using neuron labeling techniques prior to dissociation of the neurons, it is possible to examine the properties of neurons that project to different areas of the brainstem as well as more rostral brain areas (Mendelowitz and Kunze, 1991). In addition, by using anterograde neural tracers applied to the chorda tympani and/or glossopharyngeal nerves, it is possible to identify rNST neurons receiving synaptic input from these nerves (Mendelowitz *et al.*, 1992). Thus, techniques are available to examine defined populations of neurons permitting study of brainstem circuits responsible for processing taste information.

Downloaded from http://chemse.oxfordjournals.org/ by guest on October 3, 2012

ACKNOWLEDGEMENTS

This work was supported by National Institute on Deafness and Other Communication Disorders, National Institutes of Health Grant DC00288 to R.M.B.

REFERENCES

Bao, H., Bradley, R.M. and Mistretta, C.M. (1995) Development of intrinsic electrophysiological properties in neurons from the gustatory region of rat nucleus of solitary tract. *Devl. Brain Res.*, **86**, 143–154.

Bradley, R.M. and Sweazey, R.D. (1992) Separation of neuron types in the gustatory zone of the nucleus tractus solitarii based on intrinsic firing properties. *J. Neurophysiol.*, **67**, 1659–1668.

Davis, B.J. and Jang, T. (1988) A Golgi analysis of the gustatory zone of the nucleus of the solitary tract in the adult hamster. *J. Comp. Neurol.*, **278**, 388–396.

Doetsch, G.S. and Erickson, R.P. (1970) Synaptic processing of taste-quality information in the nucleus tractus solitarius of the rat. *J. Neurophysiol.*, **33**, 490–507.

Hamill, O.P., Marty, A., Neher, E., Sakmann, B. and Sigworth, F.J. (1981) Improved patch-clamp techniques for high resolution current recording from cells and cell-free membrane patches. *Pflügers Arch.*, **391**, 85–100.

Hamilton, R.B. and Norgren, R. (1984) Central projections of gustatory nerves in the rat. *J. Comp. Neurol,*. **222**, 560–577.

Kay, A.R. and Wong, R.K.S. (1986) Isolation of neurons suitable for patch-clamping from adult mammalian central nervous systems. *J. Neurosci. Methods*, **16**, 227–238.

King, C.T. and Hill, D.L. (1991) Dietary sodium chloride deprivation throughout development selectively influences the terminal field organization of gustatory afferent fibers projecting to the rat nucleus of the solitary tract. *J. Comp. Neurol.*, **303**, 159–169.

King, M.S. and Bradley, R.M. (1994) Relationship between structure and function of neurons in the rat rostral nucleus tractus solitarii. *J. Comp. Neurol.*, **344**, 50–64.

Lasiter, P.S. and Kachele, D.L. (1988) Postnatal development of the parabrachial gustatory zone in rat: dendritic morphology and mitochondrial enzyme activity. *Brain Res. Bull.*, **21**, 79–94.

Mendelowitz, D. and Kunze, D.L. (1991) Identification and dissociation of cardiovascular neurons from the medulla for patch clamp analysis. *Neurosci. Lett.*, **132**, 217–221.

Mendelowitz, D., Yang, M., Andresen, M.C. and Kunze, D.L. (1992) Localization and retention *in vitro* of fluorescently labeled aortic baroreceptor terminals on neurons from the nucleus tractus solitarius. *Brain Res.*, **581**, 339–343.

Mistretta, C.M. and Labyak, S.E. (1994) Maturation of neuron types in nucleus of solitary tract associated with functional convergence during development of taste circuits. *J. Comp. Neurol.*, **345**, 359–376.

Nakagawa, T., Shirasaki, T., Wakamori, M., Fukuda, A. and Akaike, N. (1990) Excitatory amino acid response in isolated nucleus tractus solitarii neurons of the rat. *Neurosci. Res.*, **8**, 114–123.

Newberry, N.R. and Nicoll, R.A. (1985) Comparison of the action of baclofen with *t*-aminobutyric acid on rat hippocampal pyramidal cells *in vitro*. *J. Physiol. (Lond.)*, **360**, 161–185.

Ogawa, H., Imoto, T. and Hayama, T. (1984) Responsiveness of solitario-parabrachial relay neurons to taste and mechanical stimulation applied to the oral cavity in rats. *Exp. Brain Res.*, **54**, 349–358.

Standen, N.B. and Stanfield, P.R. (1992) Patch clamp methods for single channel and whole cell recordings. In Stamford, J.A. (ed.), *Monitoring Neural Activity: A Practical Approach*. IRL Press, Oxford, pp. 59–83.

Tell, F. and Bradley, R.M. (1994) Whole-cell analysis of ionic currents underlying the firing pattern of neurons in the gustatory zone of the nucleus tractus solitarii. *J. Neurophysiol.* **71**, 479–492.

Travers, J.B. and Smith, D.V. (1979) Gustatory sensitivities in neurons of the hamster nucleus tractus solitarius. *Sens. Process.*, **3**, 1–26.

Vogt, M.B. and Mistretta, C.M. (1990) Convergence in mammalian nucleus of solitary tract during development and functional differentiation of salt taste circuits. *J. Neurosci.*, **10**, 3148–3157.

Wang, L. and Bradley, R.M. (1995) *In vitro* study of afferent synaptic transmission in the rostral gustatory zone of the rat nucleus of the solitary tract. *Brain Res.*, **702**, 188–198.

Whitehead, M.C. (1988) Neuronal architecture of the nucleus of the solitary tract in the hamster. *J. Comp. Neurol.*, **276**, 547–572.

Received on April 15, 1996; accepted on July 1, 1996

Downloaded from http://chemse.oxfordjournals.org/ by guest on October 3, 2012